AAPS PharmSciTech (2019) 20: 158
DOI: 10.1208/s12249-019-1363-6

Research Article

Insulin Mucoadhesive Liposomal Gel for Wound Healing: a Formulation with Sustained Release and Extended Stability Using Quality by Design Approach

Marwa H. S. Dawoud,[1,4] Ghada E. Yassin,[1,2] Dalia M. Ghorab,[3] and Nadia M. Morsi[3]

Received 25 January 2019; accepted 4 March 2019; published online 8 April 2019

Abstract. The present study deals with the formulation of topical insulin for wound healing with extended stability and sustained release, by applying quality by design concepts. Insulin has been promoted as a promising therapeutic wound healing agent. Topical formulation of insulin faced major problems, as it cannot be delivered safely to the wound with a controlled rate. Formulation of insulin-loaded vesicles in optimized bio-adhesive hydrogels has been explored to ensure a safe delivery of insulin to wounds in a controlled manner. Quality by design (QbD) was applied to study the effect of several critical process parameters on the critical quality attributes. Ishikawa diagram was used to identify the highest risk factors, which were screened by a fractional factorial design and augmented by Box–Behnken design. The optimized formula was incorporated into a mucoadhesive gel, which was further subjected to stability and clinical studies. An optimized formula was obtained with a particle size of 257.751 nm, zeta potential − 20.548 mv, 87.379% entrapment efficiency, and a release rate of 91.521 μg/cm^2/h. The results showed that liposomal insulin remained stable for 6 months in aqueous dispersion state at 4°C. Moreover, the release was sustained up to 24 h. The clinical study showed an improvement in the wound healing rate, 16 times, as the control group, with magnificent reduction in the erythema of the ulcer and no signs of hypoglycemia. Insulin-loaded liposomal chitosan gel showed a promising drug delivery system with high stability and sustained release.

KEYWORDS: quality by design; ishikawa diagram; insulin; liposomes; wound healing.

INTRODUCTION

Wound, specifically, chronic wounds that lasted for more than 6 months, is a major health problem, which affects the quality of life of many people. Quick wound healing with promising results became the goal of many clinical treatments. The full knowledge about wound-healing process resulted in the development of many therapies.

Insulin, a peptide hormone, with multiple physiological roles, was found to have an excellent wound-healing property, having the ability to restore the integrity of the broken skins and with a lower cost in comparison with other growth factors (1). It can stimulate keratinocyte migration and proliferation, and this effect was observed to be independent of epidermal growth factor (EGF), resulting in an epidermis with more mature morphology. It was able to accelerate wound healing by stimulating angiogenesis process and inducing a regenerative process of healing (2).

It is well known that polypeptides are complex molecules with different molecular weights ranging from 5 to 200 kDa, whose delivery has been accomplished through an invasive method as injections (3). However; these routes do not protect the protein from degradation due to proteases at the wound site and do not maintain the therapeutic levels, so they require frequent dosing. Moreover, a sustained release is required so as to lower the frequency of application, hence improving the patient compliance. Thus, continuous improvements in the formulation as well as the delivery are developed so as to formulate insulin for wound healing with increased stability and an extended release. It was found that liposomal vesicles can release peptides in a controllable manner and can protect it from the surrounding environment as peptidases (4). In addition; the use of bio-adhesive hydrogels offers additional advantages such as prolonging the residence times on the application site and reducing the frequency of product administration. Chitosan is one of the hydrogels that by its

[1] Department of Pharmaceutics, Faculty of Pharmacy, October University for Modern Sciences and Arts, (MSA University), Giza, Egypt.
[2] Department of Pharmaceutics and Industrial Pharmacy, Faculty of Pharmacy, Al-Azhar University, Cairo, Egypt.
[3] Department of Pharmaceutics and Industrial Pharmacy, Faculty of Pharmacy, Cairo University, Cairo, Egypt.
[4] To whom correspondence should be addressed. (e–mail: mdawoud@msa.eun.eg; marwa.hamdy@yahoo.com)

bio-adhesive property seals leaks stops bleeding, binds tissues, and preferably facilitates the healing process (5). Thus, formulation of insulin-loaded vesicles in an optimized bio-adhesive hydrogel could offer a controlled delivery into the wound area with promising results (6).

Food and Drug Administration (FDA) initiated the quality by design (QbD) approach; which is a strategic product development approach that puts into consideration both, product and procedure factors that affect the final quality product (7). A thorough knowledge about the process and the product is required by the pharmaceutical QbD. Moreover, the understanding of how the critical process parameters (CPP) affects the critical quality attributes (CQAs) is very important by the use of design of experiments (DoE) where, an operational design space (DS) could be established. Thus, a controlled DS could be generated for the process. The proper use of QbD will help to increase the robustness and quality of the product (8). The QbD could be summarized into four major stages: (1) creating quality target product profiles (QTPP) and CQAs, (2) risk assessment (RA), (3) design of experiments and design space establishment, and (4) control strategy with continuous improvement (8).

The present work is a case study for developing insulin liposomal chitosan gel using step-by-step QbD approach. The effects of total lipid content, phosphatidylcholine are as follows: cholesterol molar ratio and the insulin amount on the particle size, zeta potential, drug encapsulation efficiency, and the release rate were explored. A design space had been established, where, stability and clinical studies were fully studied to create a control strategy ensuring the continuation of the process with promising results for the clinical performance of the product.

MATERIALS AND METHODS

Materials

Insulin crystals were obtained as a generous gift from Sedico Company (Cairo, Egypt), L(α) phosphatidylcholine (type IV-s), and medium molecular weight chitosan were from Sigma-Aldrich (St. Louis, MO, USA), Cholesterol was from Bio Basic (Toronto, Canada). All other chemicals and solvents were of pharmaceutical grade, from ADWIC Company (Qalyubia, Egypt).

Preparation of Insulin-Loaded Liposomes

Dry thin film hydration was the method of choice used for the preparation of liposomes (9). Lipid contents (egg phosphatidylcholine and cholesterol) were added to 7.5 ml solvent mixture of chloroform and methanol, where this organic solvent was then evaporated under vacuum at the specified temperature, using rotatory evaporator (Heidolph 2, Schwabach, Germany). A dry lipid film was formed, which was collected by hydration with an insulin solution in phosphate buffer saline (PBS) (pH 6.8) by rotation for the specified time. Sonication (bath-type) was applied to the formed dispersion (Jiotech UC-10, Serangoon, Singapore) at 900 H. The preparation was left overnight for maturation.

Liposomes without insulin were prepared exactly as mentioned, but without the addition of insulin, and were additionally analyzed to act as the negative control.

Establishing Quality Paradigm

Risk Assessment (RA)

The Quality Target Product Profile (QTPP) is the properties related to the quality which a drug product needs to have to be able to achieve the requirements set in the target product profile. QTPP should achieve a quantitative substitute to describe the efficacy and clinical safety by determining the critical quality attributes (CQAs), critical process parameters (CPP), and control strategy (7). In the case of insulin loaded-liposomes, insulin with a sustained release and high stability were the main quality product profile. The risk assessment study started by listing all the factors that can affect the quality of the final product (7). The most important step in risk assessment is to sort the main factors influencing the QTPP. These factors were categorized diagrammatically using a fish-bone diagram (also known as the Ishikawa diagram or cause-and-effect diagram), which was useful in determining the main risks and accompanying causes (8). One main response, namely drug encapsulation efficiency (EE%), was defined and further delineated to identify all potential risks.

Screening Phase: Fractional Factorial Design

After risk analysis, the factors affecting the insulin entrapment efficiency were identified and found to be organic solvent volumetric ratio (chloroform: methanol) (X_1), hydration time (X_2), sonication time (X_3), and temperature of liposomes and film formation (X_4).

The first step in the screening phase was to choose a suitable experimental design, taking into consideration the number of factors to be tested and the availability of time and resources. The studied factors were studied at two different levels, low and high, as shown in Table I, which were all tested on the EE%.

Optimization Phase: Box–Behnken Design (BBD)

Based on preliminary experimental data, three critical process parameters (CPP) were selected for the Box–Behnken Design using response surface methodology (RSM) to allow the investigation of the studied CPP, namely total lipid content (X_A), phosphatidylcholine: cholesterol ratio (PC:CH) (X_B), and the insulin amount (X_C), at three different levels as shown in Table II, producing 17 runs. The impact of the CPPs was tested on the CQA, the particle size (Y_1), zeta potential (Y_2), EE% (Y_3), and the release rate (Y_4). The factors that showed a statistically significant effect, which were evaluated in the screening design, were set fixed at the level that achieves the highest EE% in Box–Behnken design.

Table I. Fractional Factorial Design Levels, Composition, and EE% Results Used in the Screening Study

Factor				Levels	
				Low (−1)	High (+1)
X_1	Solvent ratio (chloroform: methanol)			1:1	3:1
X_2	Hydration time (min)			15	60
X_3	Sonication time (min)			0	60
X_4	Temperature (°C)			45	65
Formulation code	Chloroform: methanol (*V*/V) (X_1)	Hydration time (min) (X_2)	Sonication time (min) (X_3)	Temperature (°C) (X_4)	EE% ± S.D.
S_1	−1.00	−1.00	1.00	1.00	34.26 ± 1.63
S_2	1.00	−1.00	1.00	−1.00	23.48 ± 0.98
S_3	−1.00	1.00	1.00	−1.00	34.98 ± 0.79
S_4	1.00	−1.00	−1.00	1.00	44.28 ± 3.28
S_5	−1.00	−1.00	−1.00	−1.00	53.2 ± 0.91
S_6	1.00	1.00	1.00	1.00	17.02 ± 3.54
S_7	−1.00	1.00	−1.00	1.00	78.41 ± 0.75
S_8	1.00	1.00	−1.00	−1.00	63.05 ± 2.88

Characterization of the Prepared Insulin-Loaded Liposomes

Morphology of the Prepared Liposomes

Scanning electron microscope (JSM-5600LV, JEOL Ltd., Tokyo, Japan) and binocular light optical microscope (Leica Imaging Systems, Cambridge, UK) were used to test the morphology of the vesicles. Samples for scanning electron microscope were coated with platinum before analysis. The images were obtained with a scintillating secondary electron detector with an accelerating potential of 15 keV (10).

Determination of Encapsulation Efficiency (EE%)

For EE% determination, 1 mL of the liposomal dispersion was centrifuged at 14,000 rpm for the separation of the unentrapped insulin from the entrapped one, at a temperature 4°C for 1 h in a cool centrifuge (Megafuge 16R, Hanau, Germany). The formed precipitate was washed with phosphate buffer saline (PBS) twice. The test was conducted in triplicates at least. The supernatant was assayed spectrophotometrically for the free insulin (C_f) ($\lambda_{max} = 204$ nm) (11). The percentage of entrapped insulin was calculated as follows

$$EE\% = \left[\left(C_t - C_f\right)/C_t\right] 100 \quad (1)$$

Where C_t is the initial insulin concentration, and C_f is the concentration of unentrapped insulin in the supernatant.

Particle Size and Zeta Potential Analysis

Particle size and zeta potential measurements were done using a Zetasizer (Nano-ZS90, Malvern, Worcestershire, UK), after dilution 10 times with double distilled water, at 25°C, which were all measured in triplicate and all particle size data were expressed as "mean ± SD width."

Preparation of Insulin-Loaded Liposomal Chitosan Gel

Insulin-loaded liposomal chitosan gel was formulated using a magnetic stirrer (PM010 JOAN Laboratory Hotplate Magnetic Stirrer Manufacturer, Zhejiang, China) by constantly stirring 4% *w*/*v* chitosan into 1% glacial acetic acid solution. Sonication was applied twice to remove air bubbles (12). The insulin-loaded liposomal gel was prepared by triturating the insulin-loaded liposomal dispersion with the prepared gel to form 2% gel preparation. Free insulin chitosan gel was prepared exactly the same, but instead of incorporation of insulin-loaded liposomes, free insulin solution in PBS was incorporated.

In vitro Release Study

Vertical type Franz diffusion cells (Hanson research, Los Angeles, California, USA) was used for the *in vitro* release studies with 1 cm^2 diffusion area. Insulin-loaded liposomal gel or free insulin gel was placed in the donor compartment so as to make a comparison between the release of insulin from the free gel and the insulin-loaded liposomal gel. The receptor compartment was filled with 7 mL PBS at pH 6.8, maintained at 37°C ± 0.5 and adjusted at 500 rpm. The gel was separated from the receptor compartment using cellophane membrane (Spectrum Medical Inc., Los Angeles, CA, USA cutoff 12,000–14,000) which was previously soaked in PBS overnight.

Samples were withdrawn (400 μL) at (0, 0.25, 0.5, 1, 2, 3, 4, 5, 6, 12, and 24 h), time intervals and were replaced with fresh solvent. Each formula was conducted in triplicate.

The rate of the drug release was estimated by calculating the cumulative amount of insulin released per unit area (μg/cm^2) and plotting it against time (h) for each formula, where the slope of the linear part of the graph was used to calculate the release rate (10).

Viscosity Measurement of the Optimized Insulin-Loaded Liposomal Chitosan Gel

Viscosity of the gel was measured using Brookfield viscometer at 25 ± 1°C, attached with spindle No CP42 at 10 rpm (13).

Table II. Critical Process Parameters with their Levels, the Experimental Runs and CQAs for the Prepared Insulin Liposomal Formulations

Critical process parameter				Levels			
				Low (− 1)	Medium (0)		High (1)
Total lipid content (mg) (X_A)				100	150		200
PC:CH molar ratio (X_B)				1:1	3:1		5:1
Insulin amount (IU) (X_C)				5	12.5		20
Code	(X_A)	(X_B)	(X_C)	Particle size (nm) (Y_1)	Zeta potential (mV) (Y_2)	Entrapment efficiency (%) (Y_3)	Release rate ($\mu g/cm^2/h$) (Y_4)
F_1	− 1.00	0.00	1.00	508.1 ± 5.67	− 22.9 ± 7.76	19.60 ± 3.76	52.39 ± 8.7.6
F_2	1.00	1.00	0.00	326.4 ± 3.87	− 19.6 ± 6.59	92.50 ± 4.56	138.69 ± 6.98
F_3	0.00	0.00	0.00	223.1 ± 4.98	− 21.9 ± 4.87	48.69 ± 2.71	211.12 ± 7.87
F_4	0.00	1.00	− 1.00	291.8 ± 3.76	− 20.4 ± 5.09	16.33 ± 5.12	70.97 ± 4.09
F_5	1.00	0.00	1.00	247.3 ± 4.87	− 19.5 ± 6.98	96.16 ± 4.65	120.85 ± 6.98
F_6	1.00	− 1.00	0.00	321.6 ± 5.76	− 20.9 ± 2.56	38.60 ± 2.45	75.357 ± 0.56
F_7	− 1.00	1.00	0.00	254.8 ± 3.76	− 20.5 ± 2.87	14.15 ± 7.34	44.72 ± 2.87
F_8	0.00	1.00	1.00	184 ± 3.87	− 20.6 ± 4.65	79.70 ± 4.76	170.53 ± 3.65
F_9	0.00	− 1.00	− 1.00	304.7 ± 2.76	− 21.4 ± 5.87	45.09 ± 3.65	117.16 ± 4.87
F_{10}	− 1.00	0.00	− 1.00	292 ± 3.43	− 21 ± 6.09	29.40 ± 1.78	74.843 ± 5.09
F_{11}	0.00	0.00	0.00	231.7 ± 5.65	− 21.7 ± 3.87	53.28 ± 6.54	217.88 ± 5.87
F_{12}	0.00	0.00	0.00	221.6 ± 4.12	− 20.7 ± 2.98	51.98 ± 4.76	218.44 ± 3.98
F_{13}	0.00	− 1.00	1.00	267 ± 5.23	− 21.7 ± 1.54	44.40 ± 3.89	36.96 ± 3.54
F_{14}	1.00	0.00	− 1.00	701.7 ± 6.87	− 18.8 ± 3.93	21.38 ± 2.34	119.83 ± 5.93
F_{15}	0.00	0.00	0.00	228.5 ± 2.98	− 21.9 ± 3.98	50.96 ± 4.12	196.09 ± 2.98
F_{16}	− 1.00	− 1.00	0.00	257.3 ± 4.71	− 21.8 ± 5.56	37.59 ± 2.54	89.22 ± 8.56
F_{17}	0.00	0.00	0.00	230.7 ± 4.98	− 20.7 ± 3.23	49.87 ± 5.34	196.37 ± 4.23

Data Analysis

Design-Expert 10.0.1.0® software (Stat-Ease Inc., Minneapolis, USA) was used to generate and analyze fractional factorial design, Box–Behnken design, and was used for the statistical analysis. Analysis of variance (ANOVA) and regression equations were used to analyze responses. Statistically, the best fitting experimental model being taken on the basis of comparison of coefficient of variation (CV), multiple correlation coefficient (R^2), adjusted multiple correlation coefficient (adjusted R^2), predicted residual sum of square, and graphically by 3D response surface plot provided by the program. A level of significance of p value < 0.05 was considered. The linear regression plots (observed *versus* predicted value) and normal probability curves of CQAs were plotted.

Data Optimization and Model Validation

A design space was established by analyzing the effect of each CPP on CQA, to ensure the desired quality of the product. To achieve the target, the optimization was aiming to attain the largest particle size and zeta potential, highest EE%, with the slowest release rate. Several criteria were used in the optimization of the BBD, such as overlay plot and desirability. Furthermore, the two optimized formulae with the greatest desirability, O_1 and O_2; were taken as checkpoints so as to assure the reliability of the model, by calculating the percentage bias between the expected and the observed results.

Development of Design Space of Insulin-Loaded Liposomes with Optimum Quality

The correlation between the CPP and CQAs were described in the design space. The region where the CPP could be used to obtain the required CQAs was determined, and thus establishment of the design space. It is expected that working within the design space will produce a product with the highest desired CQAs.

Determination of Control Strategy of the Optimized Insulin-Loaded Liposomes

International conference on harmonization, Q10, defines the control strategy as "a planned set of controls derived from current product and process understanding that guarantees process performance and product quality. The controls can include parameters and attributes related to drug substance and drug product materials and components, facility and equipment operating conditions, in process controls, finished product specifications and the associated methods and frequency of monitoring and control." (14). Design space determined the acceptable range of the material attributes.

Stability Studies

Insulin liposomal dispersion was tested for the stability, where, one representative formula (O_1) with highest desirability was selected with 200 mg total lipid content, 2.5:1 M ratio between PC:CH and drug amount of 20 I.U. These samples were kept at 25°C and 4°C. At predetermined time intervals, the particle size and the amount of protein remaining, by EE% measurement, were determined (as mentioned earlier) and taken as indicators for stability.

Clinical Study

The current study was conducted on 15 patients, at Ahmed Maher Hospital (Department of Dermatology, Burns and Plastic Surgery), through a period of 8 months, from

October 2016 to April 2017. A full medical history was performed on all patients, emphasizing on the cause and the duration of wound, any complications with the wound, and previous or present medication that may have an effect on the healing process in addition to the current medical conditions (*e.g.*,atherosclerosis, history of abnormal scar formation, diabetes mellitus, or history of any chronic conditions that may might have an effect on the study). The study protocol was explained to the patients before obtaining the informed consent and after approval from the ethical committees of MSA University and Cairo University. All procedures followed were in accordance with the ethical standards of Helsinki Declaration. After eligibility confirmation, patients were randomly divided into two groups (test group, 10 patients) receiving insulin-loaded liposomal chitosan gel or (control group, 5 patients) receiving liposomal chitosan gel (exactly the same as the insulin-loaded liposomal chitosan gel but without adding insulin). The package of the final working gels were each assigned a product code to ensure blindness of the study.

Inclusion Criteria. Patients with chronic wounds in different parts of the body, age between 21 to 75 years, are included in the study.

Exclusion Criteria. Patients excluded from the study are those who have severe infection (as determined by the presence of visible pus, wound exudate, redness, or warmth of the wound border), uncontrolled wound bleeding, smokers, patients with immunosuppression, cardiovascular diseases, or any chronic debilitating disease that might affect the outcome of the study.

Study Protocol. Complete general and dermatological examinations were performed, and evaluation of the wound emphasizing on the shape and wound area was conducted. Photographs of the wounds were taken at the beginning of the study and were set as the primary wound surface and shape, using digital camera. Progressive photographs were taken, where camera settings, lighting, and patient positioning were set constant at the beginning of the study, every 2 weeks for 2 months maximum, or when complete wound closure was achieved as evidenced by moist granulation tissue was no longer visible and wound area was covered by continuous layer of epithelium (15).

The topical gel was applied once daily in both test and control groups, left to dry for 30 min, and covered with sterile cotton gauze.

Erythema Measurement

Directly after absorption of the formulae from the skin, the application sites were graded according to visual scaling. The erythema scale was as follows: 0, none; 1, slight; 2, well defined; 3, moderate; and 4, scar formation, on days 0, 1, 2, 7, and 14 (16).

Wound Area Measurement

The wound area was measured by an expert physician using a sterile transparent paper; which was placed on the wound to mark wound borders. The largest two perpendicular diameters were multiplied to obtain the wound area in mm^2. The rate of wound healing was depicted from the following equation

$$(W_i - W_f)/\text{time (days)} \quad (2)$$

Where; W_i is the primary wound area and W_f is the final wound area in mm^2.

Safety Measurement

Blood glucose level was measured before application and 1 h after application of the gel in both groups. Adverse events, including headache, sweating, and vertigo (due to hypoglycemia) were reported and recorded (17).

RESULTS AND DISCUSSION

Risk Assessment

Risk assessment could be performed by risk identification and risk analysis, which are two basic components of a risk assessment study as outlined in the ICH Q9 document. The first step is to devise and enlist the whole information that can harm the whole process and plays a role in the quality of the final product, through risk identification; whereas, risk analysis focuses on the linking between the qualitative or quantitative occurrence and severity of harm (18).

The first step applied was the construction of the Ishikawa diagram as presented in Fig. 1 to identify the possible causes of product variability (19).

Drug encapsulation efficiency was found to be the highest risk factor, which is very important for both manufacturers and patients, because when it increases, reduction in the manufacturing cost could be achieved (20); furthermore, a sustained release of insulin from liposomal vesicles would be accomplished with an increase in the insulin's stability (being protected from the outer environment). Moreover, it facilitates the transport of high molecular weight protein to the skin layers (21). Accordingly, as the goal of this study was to maximize the insulin entrapment within the liposomes, thus the formulations with entrapment efficiencies of less than 5% were excluded from further analysis.

Experimental Design

Screening: 2^{4-1} Fractional Factorial Design

As shown in Table I, insulin-loaded liposomes encapsulation in the screening study varied from 17.02 to 78.41% for various prepared formulae for the screening study. The generated statistical model showed a very good correlation coefficient with a value of $(R^2) = 0.9934$. Analysis of variance (ANOVA) was used for further analysis which indicated a significant effect of the studied factors on the encapsulation efficiency ($p < 0.05$). The

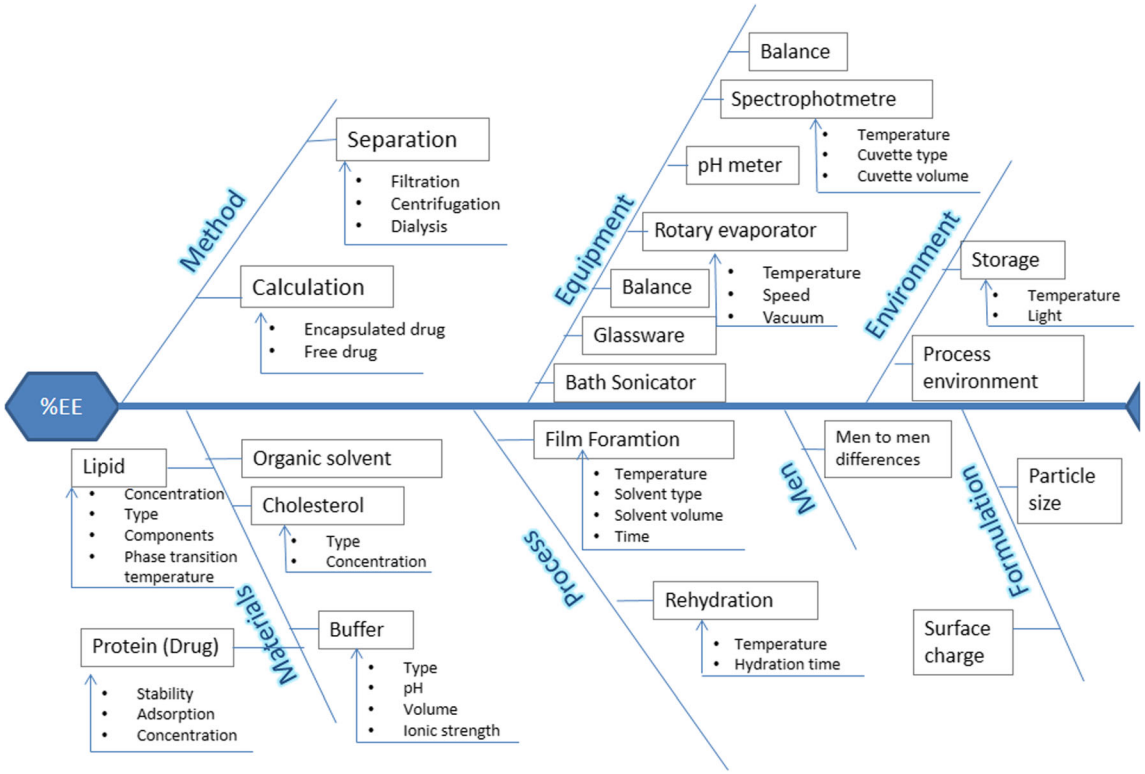

Fig. 1. Ishikawa diagram for the encapsulation efficiency of insulin-loaded liposomes

linear regression equation representing the EE% for screening is outlined in Eq. (3).

$$\%EE = +43.78 - 6.31\,X_1 + 4.70\,X_2 - 16.04\,X_3 \quad (3)$$

Out of the four investigated factors, three were statistically significant, namely solvent volumetric ratio (X_1), hydration time (X_2), and sonication time (X_3) while the effect of the temperature of liposomes and film formation (X_4) was insignificant.

As can be observed from Eq. (3), the EE% increased as the solvent volumetric ratio decreased, with a longer hydration time and without sonication, which probably could be due to the leakage of the free insulin due to sonication (22). The temperature was found to have an insignificant effect on the EE%, as the two chosen temperatures (45 and 65°C) were above the (Tc) of the liposomes, which is around 40°C (23).

The significant factors in the screening step were adjusted so as to obtain the highest EE% in the further optimization study.

Optimization of Insulin Liposomes: Box–Behnken Design

Seventeen experimental runs were conducted. Probability values (p value) by regression analysis test values were evaluated for the four critical quality attributes that have a 95% confident level. A large p value for lack of fit (>0.05) gives an indication that the lack of fit test is insignificant suggesting that the correlation between the CPP and the CQA is significant.

Particle Size

The particle size range was found to be between 701.7 and 184 nm as observed from Table II.

All CQAs and their combined actions had a significant effect on the particle size except PC:CH ratio (X_B) and its interaction between any of the total lipid content (X_{AB}) or the drug amount (X_{BC}) as represented in Table III.

The equation that represents the linear regression model for insulin-loaded liposomes of particle size, as obtained from factorial study (Table III), shows that an increase in the liposomal particle size was observed as the total lipid content increases, which may be due to the positive impact of the lipid concentration on the internal volume of the individual vesicles, which in turn may lead to the increase in their size (24). These results were in accordance with Soema *et al.* who showed that when egg phosphatidylcholine was present in high amounts, a larger vesicular size was observed. (25). Moreover, the vesicular size was observed to be smaller as the drug amount increases, as confirmed from the negative coefficient of (X_C). This could be attributed to that some of the insulin is located in the bilayers of the vesicles being amphipathic in nature (26), which leads to incorporation of the drug to the bilayers of liposomes resulting in an increase in the cohesion among the apolar portions of the membrane, thus the vesicle diameter may be reduced (10). The positive coefficient of (X_{AB}) reveals that the vesicular size of liposomes was found to increase as the total lipid amount together with the drug amount increases.

Zeta (ζ) Potential Measurement of Prepared Liposomes

Zeta (ζ) potential was found to have a negative charge at pH 6.8 as the main used component is egg

Table III. ANOVA Table for CQAs

	Source	Sum of squares	df	Mean square	*F* value	*p* value prob > F	R^2 value		Reduced regression equation
Particle size	Model (quadratic)	2.502E+005	7	35,740.45	88.68	< 0.0001	R^2	0.985	$Y_1 = +227.12+35.60$
	A total lipid	*10,138.88*	*1*	*10,138.88*	*25.16*	*0.0007*	Adj. R^2	0.974	*A−47.98* C + 1.82
	B PC:CH	*1095.12*	*1*	*1095.12*	*2.72*	*0.1337*	Pred. R^2	0.917	*A* B−167.63*A
	C drug amount	*18,412.81*	*1*	*18,412.81*	*45.69*	*< 0.0001*	Adeq. precision	35.31	*C+ 119.15*
	AB	*13.32*	*1*	*13.32*	*0.039*	*0.8489*			A^2–56.25 B^2 +
	AC	*1.124E+005*	*1*	*1.124E+005*	*278.88*	*< 0.0001*			91.00*C^2
	BC	*1228.50*	*1*	*1228.50*	*3.61*	*0.0994*			
Zeta potential	Model (linear)	10.81	3	3.60	7.61	0.0035	R^2	0.637	$Y_2 = -20.94-0.92$
	A total lipid	6.84	1	6.84	14.46	0.0022	Adj. R^2	0.553	*A−0.59 *B
	B PC:CH	2.76	1	2.76	5.83	0.0312	Pred. R^2	0.384	
	C drug amount	1.20	1	1.20	2.54	0.1352	Adeq. precision	9.064	
EE%	Model (quadratic)	9448.84	9	1049.87	73.80	< 0.0001	R^2	0.989	$Y_3 = +50.96 + 18.49$
	A total lipid	2734.30	1	2734.30	192.21	< 0.0001	Adj. R^2	0.976	*A + 4.62 *B +
	B PC:CH	171.11	1	171.11	12.03	0.0104	Pred. R^2	0.852	15.96 *C−19.34
	C drug amount	2037.07	1	2037.07	143.20	< 0.0001	Adeq. Precision	29.28	*A*B−21.15 *A
	AB	1495.37	1	1495.37	105.12	< 0.0001			*C+16.02 * B*C−5*
	AC	1788.44	1	1788.44	125.72	< 0.0001			A^2–0.25 * B^2–4.33
	BC	1025.98	1	1025.98	72.12	< 0.0001			* C^2
Release rate	Model (Quadratic)	64,327.56	8	8040.94	41.09	< 0.0001	R^2	0.897	$Y_4 = +207.98+$
	A total lipid	4682.65	1	4682.65	23.93	0.0012	Adj. R^2	0.952	24.19* A+13.28*
	B PC:CH	1410.31	1	1410.31	7.21	0.0277	Pred. R^2	0.784	B+26.96 * AB
	C drug amount	0.54	1	0.54	2.748E-003	0.9595	Adeq. precision	16.46	+44.94* B*C -
	AB	2906.99	1	2906.99	14.86	0.0048			63.96* A^2–57.03*
	AC	137.69	1	137.69	0.68	0.4384			B^2–52.05*C^2
	BC	8077.88	1	8077.88	41.28	0.0002			

phosphatidylcholine (PC) (27), which gives an indication to the presence of a weak electrostatic repulsive force between the phosphatidylcholine vesicles at pH 6.8. In addition, insulin at pH 6.8 imparts a negative charge (28). The range of the ζ potential values was − 18.8 to − 22.9 mv, which is considered a good value.

The linear regression models for insulin loaded liposomes of ζ potential, as obtained from factorial study, was represented in Table III, which shows that zeta potential absolute value increased as the total lipid content decreased. Moreover, the zeta potential was augmented as the PC:CH molar ratio was decreased. This may be attributed to the decrease in the relative amount of phosphatidylcholine, which leads to an increase in the zeta potential (25), and the subsequent increase in the cholesterol amount may increase the zeta potential, as the hydroxyl group that is present in the polar head of the cholesterol combine easily with the choline present in in the polar region of phosphatidylcholine. This will lead to production of a kind of dipole tropism that increases the liposomal surface's negative charges (29). Furthermore, the presence of the cholesterol at the bilayers might reduce the binding affinity at the surface between the cations in the buffer solution and its bilayer surface, which in turn leads to an elevated value of the negative zeta potential (27).

Encapsulation Efficiency

Encapsulation efficiency for optimization was found to be in the range of 14.15 to 96.16%. It can be deduced from Table III that the CQAs and their combined actions were significant model terms, where EE% was found to increase as any of the main factors increased as observed from their positive coefficients.

The linear regression model for insulin-loaded liposomes of EE%, as obtained from factorial study (Table III), showed that the increase in the vesicular entrapment efficiency was detected when the total lipid content was increased, which may be due to that the presence of high amount of lipid within liposomes could create more space to encapsulate more insulin within the liposomes (30). Moreover, it is known that lipid concentration positively affects the liposomal encapsulation efficiency of most hydrophilic drugs (small or large molecules), thus the insulin encapsulation may be increased by the increase in the total lipid content, owing to its effect on the total internal volume of liposomes, which is determined by the entrapment volume of individual vesicles and the total vesicle number (24).

An increase in the encapsulation efficiency was also observed as the PC:CH molar ratio increased. This may be attributed to two reasons: first, the increase in the PC content would lead to an increase in the liposomal formation and hence the EE% would increase as well (31). Second, the decrease in the cholesterol amount, as the competition between cholesterol and insulin for the packing space within the bilayer will be lowered and thus reducing the exclusion of the drug from the vesicles. However, reduction of cholesterol above a certain limit can disrupt the regular linear structure of the liposomal vesicles, thus it should be adjusted within a certain range (32).

On increasing the amount of insulin added, an increase in the insulin entrapment efficiency was observed too, which

can be observed from the positive coefficients of (X_C). This could be due to the saturation of the medium with insulin at higher concentration enforcing it to be encapsulated into liposomal vesicles (10).

The interaction between any of the studied CPP had different behavior than their individual effects; where an increase in both the total lipid content with the PC:CH molar ratio (X_{AB}) or the total lipid content with the drug amount (X_{AC}) resulted in a decrease in the entrapment efficiency, while the increase in the PC:CH together with the amount of insulin resulted in a significant increase in the EE%.

In vitro Release Rate

As can be observed from Fig. 2, a biphasic release profile was observed for the *in vitro* release of insulin. Probably, this may be attributed to the presence of the unencapsulated and encapsulated insulin, as the lipid has a small capacity to encapsulate large amounts of the drug, resulting in the deposition of the free insulin at the surface (10). The biphasic release was observed due to the presence of free protein which will be released rapidly then the entrapped insulin will be released slower and more sustained due to its diffusion through the lipid bilayers of the vesicles, thus encapsulating insulin in liposomes had a very good impact in controlling and sustaining the release of insulin (10).

The release rate was found to be from 36.96 to 218.44 μg/cm^2/h as shown in Table II and was significantly affected by all factors and their interaction except the drug amount and its combined action with the total lipid content (Table III).

It was found that the increase in the total lipid content may accelerate the release rate as can be deduced from the positive coefficient of (X_A). Furthermore, by increasing the molar ratio between the PC and cholesterol, *i.e.*, decreasing the cholesterol amount relatively, the release rate was increased. This could be attributed to the effect of cholesterol when incorporated into the bilayer, which might cause the lipid vesicles to change their packing geometrical structures as surface lipid bilayer rigidity. In addition, the Hamaker constant, van der Waals forces, electrostatic repulsive forces, and hydration forces between the lipid bilayers or lipid vesicles may all be affected following the incorporation of cholesterol into the lipid vesicles. Thus reduction in the cholesterol amount leads to a decrease in the rigidity of the vesicles thus accelerating the drug release (27).

Acceleration of the release of insulin from the liposomal vesicles was observed as a result of increase in both the total lipid content and the PC:CH, which may be due to the positive impact of each individual CPP on the release rate. Additionally, an increase in the phosphatidylcholine, cholesterol molar ratio together with the drug content, accelerated the release rate as confirmed by the positive coefficient of (X_{BC}).

Viscosity Measurement of the Optimized Insulin-Loaded Liposomal Chitosan Gel

Viscosity of the optimized insulin-loaded liposomal chitosan gel was found to be 11,404.390 ± 105.89 cp due to the presence of the insulin in the liposomes, and their incorporation into chitosan gel is considered to be very beneficial for sustaining the release of insulin (33,34).

Three-D Plots

Three-D plots of the studied CQAs were represented in Fig. 3. Analysis of 3-D plots reveals that the P.S. was decreased as the total lipid content was reduced, and the insulin amount was increased, keeping the PC:CH fixed at the two used levels till a certain point after which a remarkable increase in the particle size was observed. Moreover, decreasing the total lipid amount and PC:CH molar ratio resulted in remarkable higher zeta potential, which may be due to their individual effects. Furthermore, increasing the total lipid amount and decreasing the drug amount while fixing the (X_B), a remarkable higher EE% was observed. While the relationship between total lipid amount and PC:CH molar ratio with the release rate was not linear, their increase lead to an initial increase in the release rate followed by a slowdown.

Morphology of the Prepared Liposomes

Photomicrograph of the selected formulae were represented in Fig. 4. As can be observed, the structure of a well-identified sealed spherical vesicles, which were nearly homogenous in shape, were predominantly present with the multilamellar walls. In addition; the method of preparation was validated by the absence of fragments in the field (35).

Statistical Design and Analysis

The results of the response surface design (RSD) were analyzed using analysis of variance (ANOVA), the effect of each CPP was discussed separately, the type of each model was analyzed, and the R^2 values of each CQA were outlined in Table (III).

Statistical tests were performed to predict when a significant change occurred in the stability and the clinical tests, using GraphPad Prism®, version 5.01. (California Corporation, USA).

The "Pred R-Squared" was in reasonable agreement with the "Adj R-Squared", *i.e.*, the difference was less than 0.2. Moreover; this model could be used to navigate the design space as the adequate precision was greater than 4, indicating an adequate signal.

Data Optimization and Model Validation

Superimposing of the CQAs on a contour plot was done so as to obtain the graphical optimization. This resulted in an overlay plot as illustrated in Fig. 5 having two regions: a yellow region with accessible response values within the design space and the gray region with response values not fitting the quality product criteria. Accordingly, based on desirability criteria and overlay plot, two optimized batches (O_1 and O_2) were selected.

Determination of Control Strategy of the Prepared Insulin-Loaded Liposomes

The upper and the lower limits for the CQA and the CPP can be defined as "the control space (or normal operating ranges) where these parameters are routinely controlled during production in order to assure reproducibility"

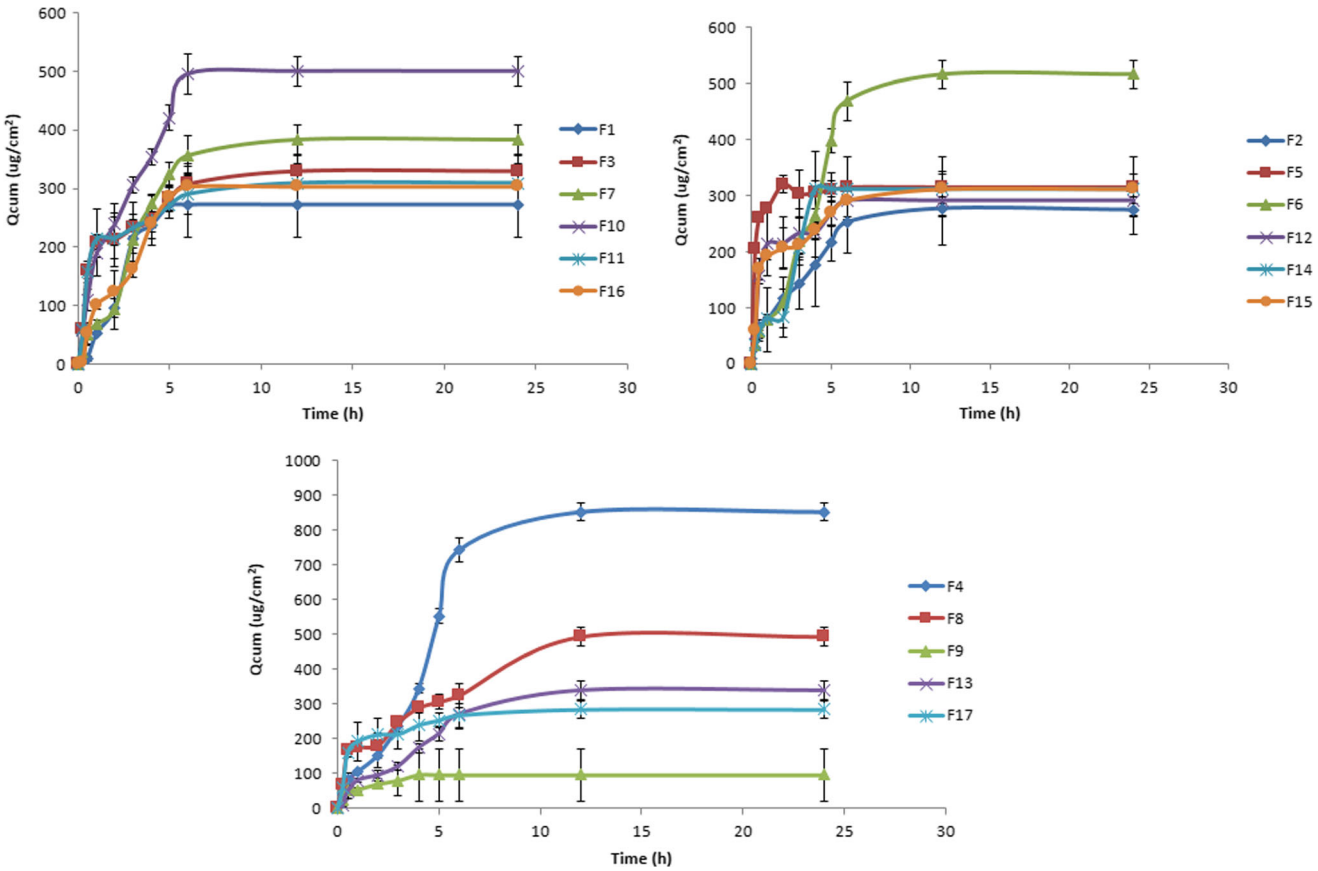

Fig. 2. *In vitro* release profiles of Insulin from insulin-loaded liposomes

(7). The control space should be within the design space. If the control space is much smaller than the design space, the process is then considered robust. Insulin-loaded liposomes satisfying these criteria were prepared and evaluated by the previously mentioned tests. The compositions of the prepared formulae were reported in Table IV, along with the observed and predicted responses. Each had three CPP, the first optimized batch (O_1) was 200 mg total lipid content, 2.5:1 M ratio between PC:CH, and drug amount of 20 I.U, with desirability 0.465; while the other (O_2) was with total lipid content of 200 mg, 2.75:1 M ratio between PC:CH, and drug amount 20 I.U, with desirability 0.463. The predicted value for particle size, zeta potential, EE%, and the release rate were respectively 257.751 nm, −20.548 mv, 87.379%, and 91.521 μg/cm^2/h for O_1 and 257.829 nm, −20.483 mv, 91.792%, and 103.307 μg/cm^2/h for O_2 in overlay plot, while the results for observed values were shown in Table IV.

The experimental observation was in reasonable agreement with the model prediction; thus, the validity of the model was established.

The release rate was comparatively evaluated for the free insulin gel and the optimized insulin-loaded liposomal gel as represented in Fig. 6, where it shows the liposomal formulation ability to sustain the release of insulin up to 24, whereas a release for 6 h only was observed with the free insulin gel.

Stability Study of Insulin-Loaded Liposomes

The stability study was performed on O_1, having higher desirability.

As shown in Fig. 7a, at 25°C, after 14 days, the particle size was increased from 219.45 to 365.7 nm followed by a dramatic significant increase in the size after 2 months to reach to 548 nm, which may be due to the flocculation of the colloidal dispersion, reflecting a poor stability of the liposomal dispersion under this temperature, owing to the increase in the thermodynamic motion of liposomes at this temperature which promotes aggregation (36). Moreover, a change in the internal arrangement of molecules inside the liposomal vesicles at high temperature may occur as self-association or aggregate formation of insulin in the liposomal membrane (37).

The results show that after 14 days, the remaining amount of the protein reached 71.71% for O_1, while after 1 month, a significant amount of insulin leaked out from the liposomes (61.66%), ensuring the instability of the liposomal dispersion at 25°C. The instability of liposomes in terms of the insulin leakage could be due to the high lipid molecular mobility at such temperature, which results in an increased lipid bilayer permeability leading to a higher protein partitioning and faster diffusion, hence, rapid protein leakage (38). Furthermore, high collision and coalescence rates of liposomal vesicles might take place, leading to particle aggregation and lipid fusion resulting in more insulin leakage. Moreover, the probability of leakage of insulin from the liposome internal aqueous compartment is less due slow diffusion, unless the integrity of the liposome bilayer is lost under stress (20).

At 4°C as represented by Fig. 7b, the particle size was found to show no significant increase in the vesicular size after 6 months (from 257.75 to 281.54 nm), which may be due to triggering the hydrolysis of the ester bonds linking the fatty acids to the glycerol in the backbone of the lipids when refrigerated (39). Also, the refrigerated conditions avoid

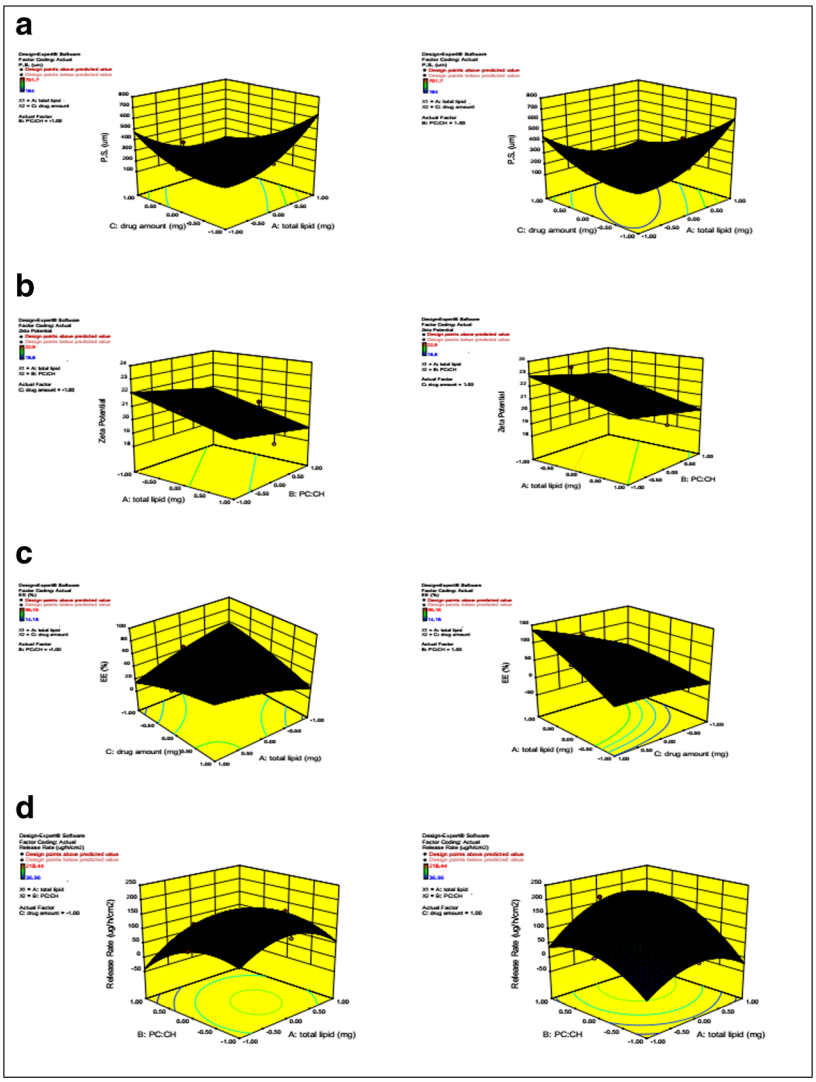

Fig. 3. Three-D plots for low and high level of the third factor for (**a**) particle size, (**b**) zeta potential, (**c**) EE%, and (**d**) release rate

hydrolysis and oxidation of the phospholipids (40). It can be observed that no significant protein leakage till 4 months for O_1 (remaining insulin encapsulated reached 86.62% after 4 months storage period). The more intense thermodynamic motion was, the easier the encapsulated protein to leak, thus liposomes supposed to be stored at 4°C (36).

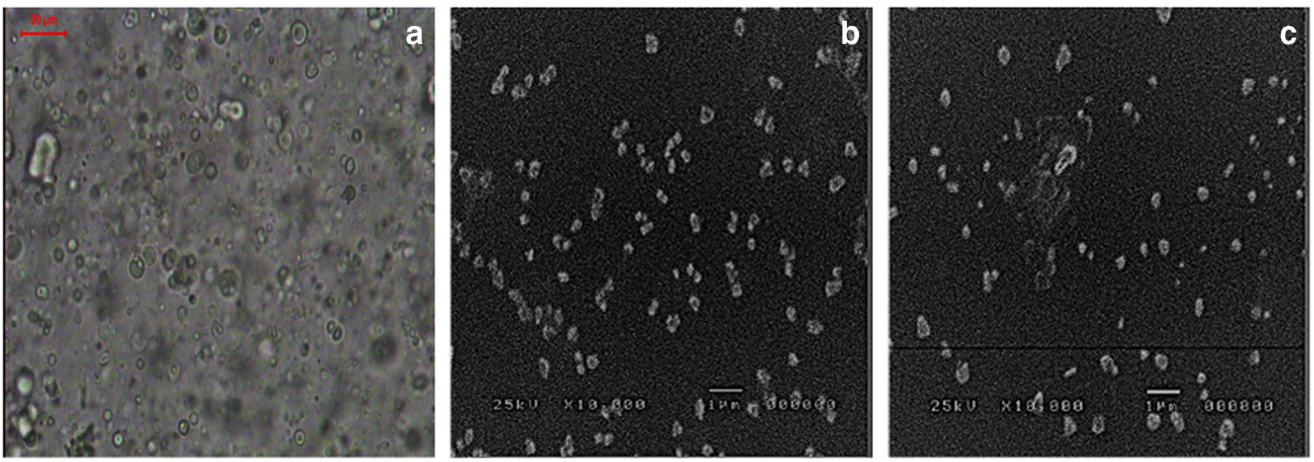

Fig. 4. Photomicrographs of the prepared liposomes using (**a**) optical microscope and (**b** and **c**) scanning electron microscope

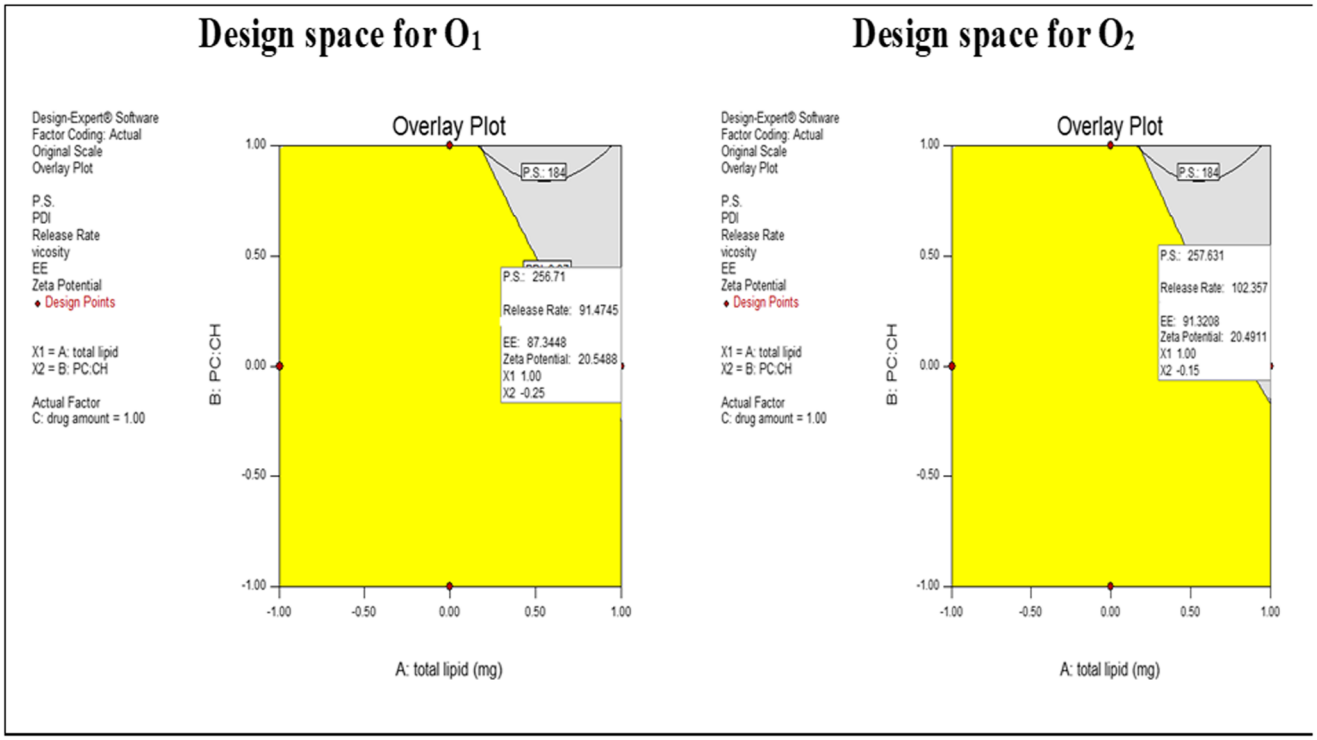

Fig. 5. Overlay plot showing the location of optimized Insulin-loaded liposomes in design space

Clinical Study

Results from the patients in the study were tabulated and expressed as mean ± standard deviation (SD), were explored using Kolmogorov–Smirnov test of normality, and were found to have parametric distribution.

Erythema Measurement. A significant change occurred at day 14 for the control group (p value < 0.05), which may be due to the anti-inflammatory effect of the chitosan. Chitosan is believed to have role in the enhancement of the inflammatory cells functions such as macrophages, polymorphonuclear leukocytes, and fibroblasts, which promotes granulation and organization (41). The test formulation showed a statistical improvement in the erythema at day 7, which may be due to the effect of the insulin as an anti-inflammatory agent due to its vasodilatory effect, where it releases endothelial nitrogen oxide (NO) in arteries, veins, and capillaries. This vasodilatation reduces leukocyte adhesion to the endothelium and subsequent infiltration. Moreover, it inhibits platelet adhesion and aggregation. Furthermore; insulin suppresses three important inflammatory mediators: intercellular cell adhesion molecular-1 (ICAM-1), monocyte chemoattractant protein-1 (MCP-1) expression, and nuclear factor kappa B (NFκB) binding in human aortic endothelial cells *in vitro*. These effects could be blocked by nitrogen oxide inhibitor N(G)-nitro-L-arginine, indicating the effects are mediated by nitrogen oxide release. Tumor necrosis factor alpha pro-inflammatory cytokines is considered the most active one in triggering the production of other cytokines such as interleukine-6 (IL-6) and other expression molecules (42).

By comparing the control group with the test group, no significant difference among the groups was observed (p value = 0.1172), the only observed change is that insulin accelerated the erythema disappearance only.

Table IV. The Predicted, Observed and Residual Values of the two Optimized Formulae

	CQA	Predicted	Observed	% Biased*
	Particle size (nm)	256.751	219.45	11.9002
O_1	Z.P. (mv)	− 20.548	− 22.3	− 7.8565
$X_1 = 1.000$	EE (%)	87.390	83.56	4.583533
$X_2 = -0.247$	Release rate (μg/cm^2/h)	91.521	95.876	− 4.50999
$X_3 = 1.000$				
	Particle size (nm)	257.829	237.85	8.399832
O_2	Z.P. (mv)	− 20.483	− 21.3	− 3.83568
$X_1 = 1.000$	EE (%)	91.792	89.98	2.013781
$X_2 = -0.136$	Release rate (μg/cm^2/h)	103.307	107.787	− 4.15635
$X_3 = 1.000$				

% Biased, (predicted-observed)/observed
O_1 and O_2 represent the optimized formulae as obtained from RSM study

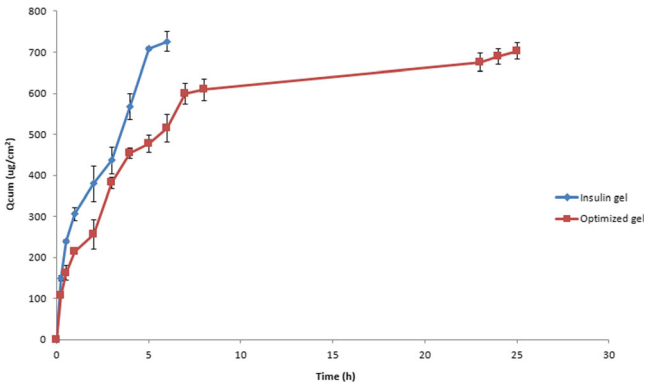

Fig. 6. Cumulative amount of Insulin released from free Insulin chitosan gel and optimized Insulin liposomal chitosan gel

Rate of Wound Healing. It could be observed from Fig. 8 that the control group produced a moderate significant change after 8 weeks with a healing rate of 2.27 ± 1.034 mm^2/day, while the test group showed a healing rate of 36.67 ± 12.179 mm^2/day with a significant change in the wound area at the 4th week. A highly significant difference was observed between the control and the test group. It can be observed that the rate of wound healing of the test was about 16 times (highly significant) the control. It should be noted that a highly significant increase between the control and the test group was observed. The control group showed a good healing process due to the presence of chitosan, while the test group showed a dramatic improvement, which may be due to the anabolic action of insulin as a growth factor in healing events, where, insulin acts on growth hormone receptors and increases reepithelialization as well as collagen content, granulation tissue, wound tensile strength, and local production of insulin-like growth factors by fibroblasts (43). Insulin also stimulates proliferation and migration of human keratinocytes, which stimulates cell growth and enhances wound healing (44).

Safety Evaluation. No significant adverse drug events or reactions were observed, and none of the participants experienced adverse systemic effects such as hypoglycemia, vertigo, sweating, and headache related to insulin administration. Blood glucose levels did not differ between treatment groups or following application of the treatment. No wound infection or uncontrolled wound bleeding occurred during the treatment period, and none of the subjects had local pain, thus ensuring the safety of the prepared formulation.

CONCLUSION

The present study describes how the QbD approach was adopted for the development of liposomal insulin with enhanced stability and sustained release to be used in wound healing. The effects of CPP on CQA were assessed using Box–Behnken design for achieving the desired QTPP.

Insulin found a solution to its instability and uncontrollable release, by formulating it into a liposomal chitosan gel. The liposomal dispersion remained stable for at least 6 months in aqueous dispersion state at 4°C, and the protective ability of liposomes on insulin was proven. The formulation was applied once daily, which improves patient's compliance, especially with the painful wounds. Moreover. the clinical

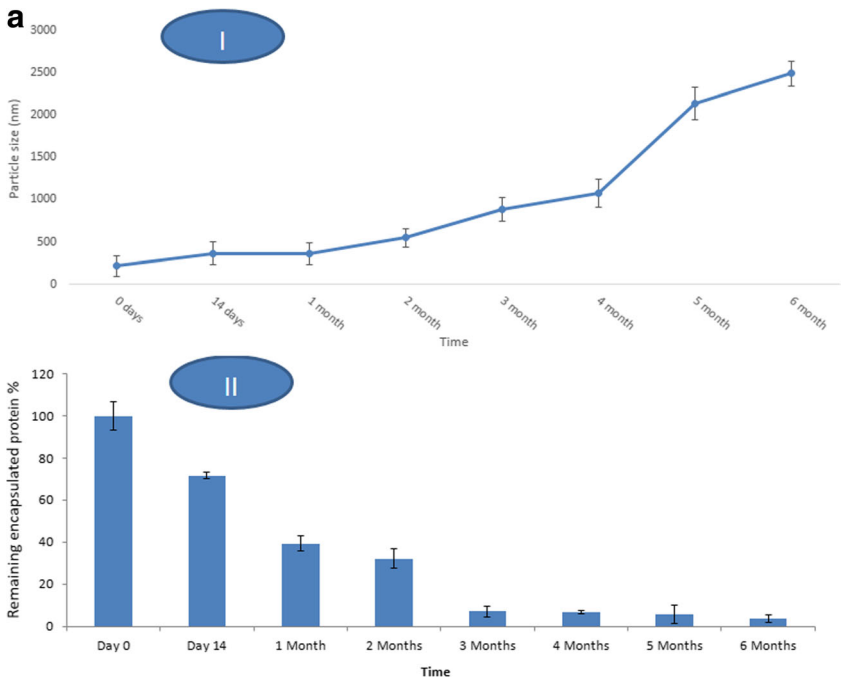

Fig. 7. **a** Liposome storage stability at 25°C. (I) Particle size and distribution width (shown as error bar and (II) remaining encapsulated protein% (mean ± SD). **b** Liposome storage stability at 4°C. (I) Particle size and distribution width (shown as error bar) and (II) remaining encapsulated protein% (mean ± SD)

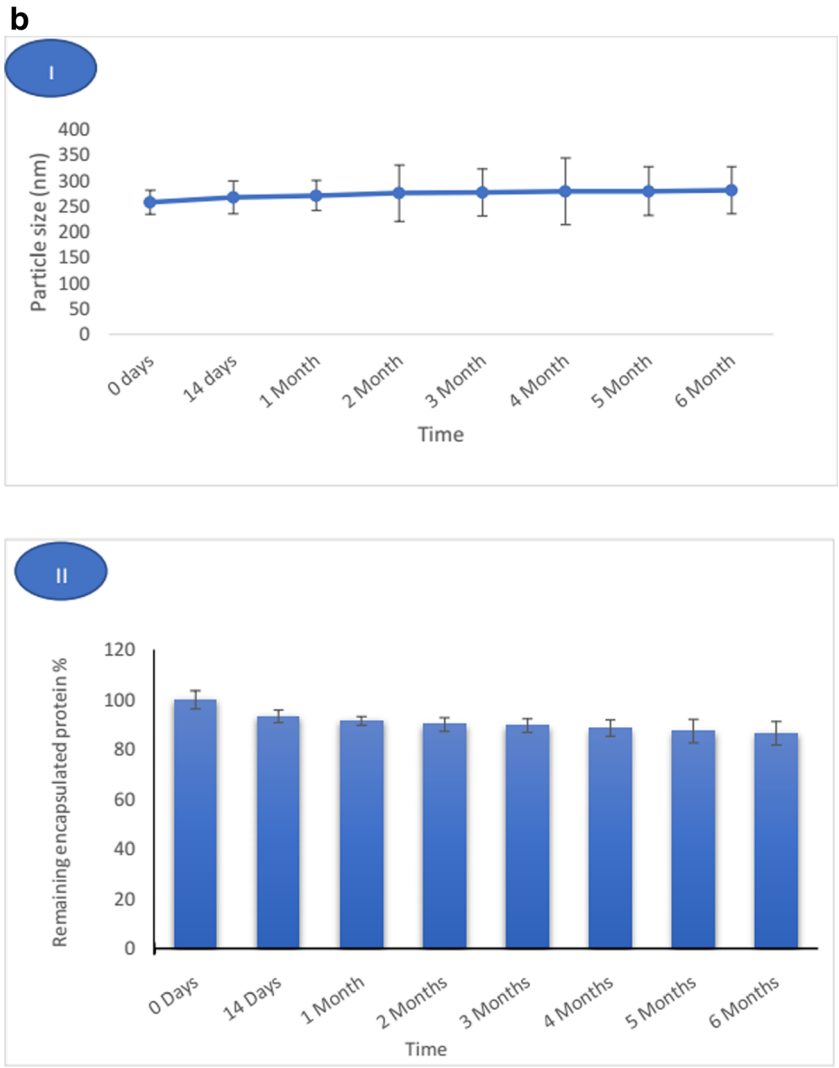

Fig. 7. (continued)

study showed outstanding results, reducing the erythema and the duration to wound healing, with an increase in the wound healing rate to about 16 times as the control formula. The insulin-loaded liposomal chitosan gel offered a very good solution to the problems of insulin, by the use of the successful quality by design concepts to achieve the best quality attribute with a strategy to continuous improvement.

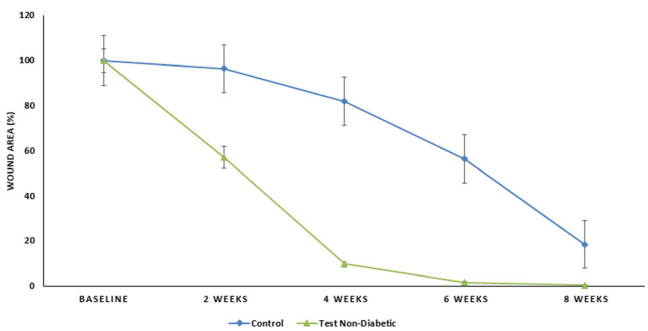

Fig. 8. Wound area quantified every 2 weeks and expressed as the percentage of the original wound area

ACKNOWLEDGMENTS

This work was supported by the October University for Modern Sciences and Arts (MSA), Egypt.

COMPLIANCE WITH ETHICAL STANDARDS

The study protocol was explained to the patients before obtaining the informed consent and after approval from the ethical committees of MSA University and Cairo University. All procedures followed were in accordance with the ethical standards of Helsinki Declaration.

Conflict of Interests Marwa H.S. Dawoud, Nadia M. Morsi, Dalia M. Ghorab, and Ghada E. Yassin declare that the insulin-liposomal is registered in the Egyptian patency office (1072/2017). However, this does not alter the authors' adherence to all the journal's policies on sharing data and materials. This research did not receive any specific grant from funding agencies in the public, commercial, or not-for-profit sectors.

REFERENCES

1. Joseph B. Insulin in the treatment of non-diabetic bed sores. Ann Surg. 1930;92(2):318–9.
2. Liu Y, Petreaca M, Martins-Green M. Cell and molecular mechanisms of insulin-induced angiogenesis. J Cell Mol Med. 2009;13(11–12):4492–504.
3. Chen S, Singh J. Controlled release of growth hormone from thermosensitive triblock copolymer systems: in vitro and in vivo evaluation. Int J Pharm. 2008 [cited 2016 Aug 18];352(1):58–65.
4. Ulrich A. Biophysical aspects of using liposomes as delivery vehicles. Biosci Rep. 2002 [cited 2016 Aug 18];22(2):129–50.
5. Parente ME, Andrade AO, Ares G, Russo F. Bioadhesive hydrogels for cosmetic applications. Int J Cosmet Sci. 2015;37(5):511–8.
6. AbdelKader DH, Osman MA, Elgizaway SA, Faheem A, McCarron PA. The role of insulin in wound healing process : mechanism of action and pharmaceutical applications. J Anal Pharm Res. 2016;2(1).
7. Patwardhan K, Asgarzadeh F, Dassinger T, Albers J, Repka MA. A quality by design approach to understand formulation and process variability in pharmaceutical melt extrusion processes. J Pharm Pharmacol. 2015;67(5):673–84.
8. Yu LX. Pharmaceutical quality by design: product and process development, understanding, and control. Pharm Res. 2008;25(4):781–91.
9. Hülsermann U, Hoffmann M. Uptake of apolipoprotein E fragment coupled liposomes by cultured brain microvessel endothelial cells and intact brain capillaries. J drug drug Target. 2009;17(8):610–8.
10. Aboelwafa AA, El-Setouhy DA, Elmeshad AN. Comparative study on the effects of some polyoxyethylene alkyl ether and sorbitan fatty acid ester surfactants on the performance of transdermal carvedilol proniosomal gel using experimental design. AAPS PharmSciTech. 2010 Dec [cited 2013 Nov 28];11(4):1591–602.
11. Xu X, Khan MA, Burgess DJ. A quality by design (QbD) case study on liposomes containing hydrophilic API: I. Formulation, processing design and risk assessment. Int J Pharm. Elsevier B.V. 2011;419(1–2):52–9.
12. Sezer AD, Hatipoğlu F, Cevher E, Oğurtan Z, Baş AL, Akbuğa J. Chitosan film containing fucoidan as a wound dressing for dermal burn healing: preparation and in vitro/in vivo evaluation. AAPS PharmSciTech. 2007;8(2):Article 39.
13. Ranade S, Bajaj A, Londhe V, Babul N, Kao D. Fabrication of topical metered dose film forming sprays for pain management. Eur J Pharm Sci. 2017;100:132–41.
14. Pogány J. ICH pharmaceutical quality system Q10. WHO Drug Inf. 2008;22(3):177–81.
15. Matuszewska B, Keogan M, Fisher DM, Soper KA, Hoe CM, Huber AC, et al. Acidic fibroblast growth factor: evaluation of topical formulations in a diabetic mouse wound healing model. Pharm Res. 1994;11(1):65–71.
16. Elsner P, Wilhelm D, Maibach H. Multiple parameter assessment of vulvar irritant contact dermatitis. Contact Dermatitis. 1990;23(1):20–6.
17. Rezvani O, Shabbak E, Aslani A, Bidar R, Jafari M, Safarnezhad S. A randomized, double-blind, placebo-controlled trial to determine the effects of topical insulin on wound healing. Ostomy Wound Manage. 2009;55(8):22.
18. ICH Expert Working Group. Quality risk management Q9. In: ICH harmonised tripartite guideline. 2005. p. 1–23.
19. Shah B, Khunt D, Bhatt H, Misra M, Padh H. Application of quality by design approach for intranasal delivery of rivastigmine loaded solid lipid nanoparticles: effect on formulation and characterization parameters. Eur J Pharm Sci Elsevier BV. 2015;78:54–66.
20. Xu X, Costa AP, Khan MA, Burgess DJ. Application of quality by design to formulation and processing of protein liposomes. Int J Pharm Elsevier BV. 2012;434(1–2):349–59.
21. Maestrelli F, González-Rodríguez ML, Rabasco AM, Mura P. Effect of preparation technique on the properties of liposomes encapsulating ketoprofen-cyclodextrin complexes aimed for transdermal delivery. Int J Pharm. 2006;312(1–2):53–60.
22. Ahad A, Aqil M, Kohli K, Sultana Y, Mujeeb M, Ali A. Formulation and optimization of nanotransfersomes using experimental design technique for accentuated transdermal delivery of valsartan. Nanomedicine Elsevier Inc. 2012;8(2):237–49.
23. Li J, Wang X, Zhang T, Wang C, Huang Z, Luo X, et al. A review on phospholipids and their main applications in drug delivery systems. Asian J Pharm Sci Elsevier Ltd. 2014;10(2):81–98.
24. Xu X, Costa A, Burgess DJ. Protein encapsulation in unilamellar liposomes: high encapsulation efficiency and a novel technique to assess lipid-protein interaction. Pharm Res. 2012;29(7):1919–31.
25. Soema PC, Willems GJ, Jiskoot W, Amorij JP, Kersten GF. Predicting the influence of liposomal lipid composition on liposome size, zeta potential and liposome-induced dendritic cell maturation using a design of experiments approach. Eur J Pharm Biopharm Elsevier BV. 2015;94:427–35.
26. Tabbakhian M, Rogers JA. Interaction of insulin, cholesterol-derivatized mannan, and carboxymethyl chitin with liposomes: a differential scanning calorimetry study. Res Pharm Sci. 2012;7(1):43–50.
27. Liu DZ, Chen WY, Tasi LM, Yang SP. Microcalorimetric and shear studies on the effects of cholesterol on the physical stability of lipid vesicles. Colloids Surfaces A Physicochem Eng Asp. 2000;172(1–3):57–67.
28. Brange J, Langkjoer L. Insulin structure and stability. Pharm Biotechnol. 1993;5(1922):315–50.
29. Xia S, Xu S. Ferrous sulfate liposomes: preparation, stability and application in fluid milk. Food Res Int. 2005;38(3):289–96.
30. Zhang X, Qi J, Lu Y, Hu X, He W, Wu W. Enhanced hypoglycemic effect of biotin-modified liposomes loading insulin: effect of formulation variables, intracellular trafficking, and cytotoxicity. Nanoscale Res Lett. 2014;9(1):1–10.
31. Yang S, Chen J, Zhao D, Han D, Chen X. Comparative study on preparative methods of DC-Chol/DOPE liposomes and formulation optimization by determining encapsulation efficiency. Int J Pharm Elsevier BV. 2012;434(1–2):155–60.
32. Moghddam SRM, Ahad A, Aqil M, Imam SS, Sultana Y. Formulation and optimization of niosomes for topical diacerein delivery using 3-factor, 3-level Box-Behnken design for the management of psoriasis. Mater Sci Eng C Elsevier BV. 2016;69:789–97.
33. Elnaggar YSR, El-Refaie WM, El-Massik MA, Abdallah OY. Lecithin-based nanostructured gels for skin delivery: an update on state of art and recent applications. J Control ReleaseElsevier B**V**. 2014;180(1):10–24.
34. Bhardwaj TR, Kanwar M, Lal R. Drug development and industrial pharmacy natural gums and modified natural gums as sustained-release carriers. Drug Dev Ind Pharm. 2000;26(768506750):1025–38.
35. López-Pinto JM, González-Rodríguez ML, Rabasco AM. Effect of cholesterol and ethanol on dermal delivery from DPPC liposomes. Int J Pharm. 2005;298(1):1–12.
36. Wang H, Liu M, Du S. Optimization of madecassoside liposomes using response surface methodology and evaluation of its stability. Int J Pharm Elsevier BV. 2014;473(1–2):280–5.
37. El-Samaligy MS, Afifi NN, Mahmoud EA. Evaluation of hybrid liposomes-encapsulated silymarin regarding physical stability and in vivo performance. Int J Pharm. 2006;319(1–2):121–9.
38. Xu X, Khan MA, Burgess DJ. A quality by design (QbD) case study on liposomes containing hydrophilic API: II. Screening of critical variables, and establishment of design space at laboratory scale. Int J Pharm. Elsevier B.V. 2012;423(2):543–53.
39. Kanta S, Plangklang B, Subsingha W. Atherosclerotic Cardiovascular Ddisease. Energy Procedia. 2011;56:604–9.
40. Casals E, Galán AM, Escolar G, Gallardo M, Estelrich J. Physical stability of liposomes bearing hemostatic activity. Chem Phys Lipids. 2003;125(2):139–46.
41. Berardesca E, Iorizzo M, Abril E, Guglielmini G, Caserini M, Palmieri R, et al. Clinical and instrumental assessment of the effects of a new product based on hydroxypropyl chitosan and

potassium azeloyl diglycinate in the management of rosacea. J Cosmet Dermatol. 2012;11(1):37–41.
42. Sun Q, Li J, Gao F. New insights into insulin: the anti-inflammatory effect and its clinical relevance. World J Diab. 2014;5(2):89–96.
43. Thalhimer W. Insulin treatment of postoperative (nondiabetic) acidosis. J Am Med Assoc. 1923;81(5):383–5.
44. Sahu K, Sharma M, Bansal H. Topical photodynamic treatment with poly- L -lysine – chlorin p6 conjugate improves wound healing by reducing hyperinflammatory response in pseudomonas aeruginosa -infected wounds of mice. Lasers Med Sci. 2013;28(2):465–71.